Pirfenidone prevents esophageal stricture by inhibiting nucleotide binding oligomerization domain like receptor protein 3 inflammasome activation

Shinji Hirano, Akira Higashimori, Yasuaki Nagami, Yuji Nadatani, Tetsuya Tanigawa, Masaki Ominami, Shusei Fukunaga, Koji Otani, Shuhei Hosomi, Fumio Tanaka, Noriko Kamata, Koichi Taira, Toshio Watanabe, Yasuhiro Fujiwara

Abstract

Background and Aim: Esophageal injury often results in a scar, leading to refractory strictures. The NLRP3 inflammasome activates caspase-1, causing the maturation of interleukin (IL)-1β. Here, we aimed to investigate the preventive effect of pirfenidone (PFD), an antifibrotic drug, on esophageal stricture after ulcer healing and studied its mechanism by focusing on the activation of the NLRP3 inflammasome.

Methods: Esophageal ulcers were induced in rats via the local application of acetic acid in the serosa. PFD was intraperitoneally administered to the rats 3 days after ulcer induction. The effect of PFD on esophageal stricture after ulcer healing was assessed by esophagography on day 9. The protein levels of mature caspase-1 and IL-1β were assessed by western blotting.

Results: The ulcers fully developed 3 days after induction and were almost scarred by day 9 with severe strictures. PFD promoted ulcer healing and attenuated fibrotic collagen in the submucosa by suppressing the increase in NLRP3, cleaved caspase-1, and mature IL-1β expression, improving stricture rate (PFD vs. vehicle = 55% vs. 81%). Exogenous IL-1β abolished the therapeutic effects of PFD on ulcer healing and stricture formation. Furthermore, NLRP3 and caspase-1 inhibitors mimicked the effects of PFD on ulcer healing and stricture formation, with suppression of the increase in cleaved caspase-1 and mature IL-1β proteins and expression of fibrosis-related molecules including transforming growth factor (TGF)-β1.

Conclusion: The NLRP3 inflammasome promotes esophageal stricture formation following ulcer healing, and PFD exerts potential prophylactic activity against strictures, possibly via the inhibition of the NLRP3/IL-1β/TGF-β1 axis.

Keyword: pirfenidone, esophageal stricture, ulcer healing, inflammasome, interleukin-1β

Text

Introduction

An esophageal stricture has negative effects on the quality of life of patients and may lead to severe complications.[1] It has several potential etiologies, including gastroesophageal reflux diseases,[2] eosinophilic esophagitis,[3] and post-endoscopic therapy.[4] In particular, the incidence of esophageal stricture after endoscopic treatment for early esophageal cancer has recently increased and become a major problem.[5] In order to prevent esophageal stricture, prophylactic procedures including balloon dilation, local steroid injection, and oral steroids have been used.[6–8] However, new treatments should be developed from a different perspective, as the current therapies do not completely prevent strictures.

Esophageal stricture is caused by the formation of scars associated with esophageal injury and biomechanical deterioration due to excessive fibrosis in the submucosa.[9–11] Scar formation is an integral part of wound healing, which starts with inflammation and is followed by cell proliferation and fibrosis.[12] Although a variety of fibrosis-related molecules, including transforming growth factor (TGF)-β and collagens, are upregulated during esophageal ulcer healing,[13–18] the regulatory mechanisms and roles of these molecules remain unclear.

The inflammasome is an important component of the innate immune response. Depending on the type of stimulus, various nucleotide-binding and oligomerization domain-like receptor (NLR) proteins constitute the inflammasome, which can regulate the secretion of interleukin (IL)-1β and IL-18 in response to an individual stimulus.[19] Inflammasome signaling and downstream cytokine responses mediated by the inflammasome play an important role in fibrosis. Studies have confirmed the role of the NLR pyrin domain

containing 3 (NLRP3) inflammasomes in driving collagen deposition in tissues and activating caspase-1 in various inflammatory and fibrotic diseases such as lung, liver, heart, and kidney diseases.[20–23]

Pirfenidone (PFD) is a pyridone analog (5-methyl-1-phenyl-2-(1H)-pyridone) used in the treatment of idiopathic pulmonary fibrosis.[24] PFD exhibits antifibrotic activity as well as anti-inflammatory and anti-oxidant activities in other progressive fibrotic and inflammatory disorder models, including esophageal burn and inflammatory bowel disease models.[16,25,26] Recent studies have suggested that PFD suppresses fibrosis in pulmonary, renal, and cardiac disorders by inhibiting inflammasome activation.[27–29] However, to our knowledge, there is no study on the role of PFD and inflammasomes in esophageal ulcer healing and stricture. Here, we aimed to clarify whether PFD can be used as prophylaxis for esophageal strictures during ulcer healing, using a rat artificial ulcer model. We also clarified the role of the NLRP3 inflammasome pathway in esophageal stricture formation following ulcer healing.

Methods

Animals

Specific-pathogen-free 8-week-old male Sprague–Dawley rats were obtained from Japan SLC, Inc. (Shizuoka, Japan). The rats fasted for 12 h were subjected to laparotomy under inhalation anesthesia with isoflurane (4.0 L/min for induction, 2.0 L/min for maintenance), and all efforts were made to minimize suffering to the rats. All experiments were performed under the supervision of the Animal Research Committee in accordance with the relevant guidelines. All experimental procedures were approved by the Animal Care Committee of our institution (Approval number 19018). We repeated the entire set of rat

experiments at least twice on different days.

Induction of experimental esophageal ulcers in rats

Esophageal ulcers were induced using the method described by Tsuji et al. and Baatar et al.,[14,30] with some modifications. Briefly, after careful separation of vessels and nerves, 100% acetic acid (30 μL) was applied to the serosa of the lower esophagus through a polyethylene tube with an oval tip (inner long diameter, 6 mm; inner short diameter, 3 mm) for 3 min. The serosa was subsequently washed with normal saline, and the abdomen was closed. Non-operated rats were used as controls for molecular biological analysis. For the subsequent experiments, the rats were euthanized in the ulcer formation stage (day 3), healing stage (day 6), and healing completion stage (day 9), according to a previous study.[14] The ulcer area was measured using a computerized image-analysis system (Image J/FL; Universal Imaging Corp., Westchester, PA) as previously described.[13,31]

Reagents

PFD (100, 250, or 500 mg/kg; Shionogi & Co., Ltd., Osaka, Japan) suspended in 0.5% carboxymethylcellulose solution or vehicle was intraperitoneally administered to the rats with esophageal ulcers. To evaluate the role of the NLRP3 inflammasome, some rats were intraperitoneally administered the NLRP3 inhibitor glyburide (10 mg/kg; Novus Biologicals, LLC, Centennial, CO), the caspase-1 inhibitor ac-YVAD-cmk (3 mg/kg; Merck K GaA, Darmstadt, Germany), or rat recombinant IL-1β (0.1 μg/kg; R&D Systems, Inc., Minneapolis, MN). All reagents were administered once daily starting on day 3.

Measurement of esophageal stricture

The esophageal stricture was measured by esophagography before sacrificing the rats on day 9, as reported previously.[15] The stricture rate was calculated as 100 × (A–B) / A,

where A is the largest diameter on the oral side of the esophagus and B is the narrowest diameter of the esophagus after filling the esophagus with the contrast medium. We repeated esophagography five times per rat and used the average value as the esophageal diameter of the individual.

Measurement of esophageal fibrosis

Paraffin-embedded esophagus specimens, cut longitudinally at the center of the ulcer, were cut into 4-μm-thick slices and stained with Masson trichrome for fibrosis evaluation. At equal magnification, the thickness and area of fibrosis were measured. The area of fibrosis was calculated using ImageJ as the percentage of blue-stained areas.

Real-time quantitative reverse transcription polymerase chain reaction

Real-time quantitative reverse transcription-polymerase chain reaction (qRT-PCR) was performed using TaqMan Fast Universal PCR master mix (Thermo Fisher Scientific Inc., Waltham, MT) on a 7500 Fast Real-Time PCR system (Thermo Fisher Scientific Inc.) as described previously.[32] Glyceraldehyde-3-phosphate dehydrogenase (GADPH) was used as the reference gene. The mRNA levels are expressed as a percent of the mean value for rats in the untreated control group. The primers and probes used are listed in Supplementary Table 1.

Western blotting

The esophageal tissues were homogenized and lysed in ice-cold lysis buffer. Proteins were separated by sodium dodecyl sulfate-polyacrylamide gel and transferred onto polyvinylidene fluoride membranes as described previously.[33] The blots were immunostained with primary antibodies and appropriate secondary antibodies. The antibodies used and their dilutions are listed in Supplementary Table 2.

Immunofluorescence studies

The esophageal specimens were fixed with 4% paraformaldehyde phosphate buffer solution for 120 min at 4°C and cryoprotected overnight in phosphate-buffered saline containing 20% sucrose. The tissues were frozen in OCT compound (Sakura FineTek Japan, Tokyo, Japan) and sectioned on a cryostat (Thermo Fisher Scientific Inc.). The samples were then incubated with primary antibodies and reacted with the corresponding secondary fluorescent dye-conjugated antibodies (Invitrogen Corporation, Carlsbad, CA). Images were captured by fluorescent microscopy. The antibodies used and their dilutions are listed in Supplementary Table 2.

Statistical analysis

GraphPad Prism 7 (GraphPad Software, San Diego, CA) was used for statistical analysis. Values are expressed as mean ± standard deviation. An independent Student's *t*-test was used to compare the differences between the groups. The one-way analysis of variance was used to compare the differences among multiple groups, and the results were analyzed using Tukey's multiple comparisons test. Statistical significance was set at $P < 0.05$.

Results

Dynamics of ulcer healing and subsequent induction of stricture

The esophageal ulcer area reached the maximum on day 3 after ulcer induction; thereafter, it gradually decreased. The ulcers almost healed macroscopically, and strictures were observed in esophagography on day 9 (Fig. 1A-C). Microscopically, on day 3, the esophageal ulcers were visualized as deep necrotic lesions involving the esophageal mucosa, submucosa, and muscularis propria (Fig. 1D). On day 6, a thin sheet of squamous epithelial cells migrated from the ulcer margin onto the granulation tissue to partially

cover the ulcer base (Fig. 1E). On day 9, macroscopically healed esophageal ulcers were mostly re-epithelialized, and the volume of the submucosal layer was increased (Fig. 1F).

Expression of cytokines and fibrosis-related molecules during ulcer healing

The mRNA expression of tumor necrosis factor (TNF)-α (Supplementary Fig. 1A) and IL-6 (Supplementary Fig. 1B) in the esophageal tissue peaked on day 3 and gradually diminished on days 6 and 9, showing similar dynamics as the esophageal ulcer area (n = 8). In contrast, the mRNA levels of IL-1β (Fig. 1G), NLRP3 (Fig. 1H), caspase-1 (Fig. 1I), TGF-β1 (Fig. 1K), and collagen type I alpha 1 chain (COL1A1) (Fig. 1L) peaked on day 6 and decreased on day 9. Ulceration did not influence IL-18 mRNA expression (Fig. 1J) during the study (n = 8).

PFD promotes ulcer healing

The ulcer areas in the rats treated with 500 mg/kg PFD significantly decreased by 31% compared with those in the vehicle-treated rats on day 6 (n = 8) (Fig. 2A). Consequently, we identified 500 mg/kg as an effective dose, and the subsequent experiments were conducted with 500 mg/kg PFD. The body weight of the rats continued to decrease until day 3. After day 4, the body weight of the PFD-treated rats gradually increased; however, the body weight of the vehicle-treated rats did not recover to the basal control levels during the study (n = 8) (Fig. 2B). Treatment with PFD in untreated rats did not affect body weight change by day 9 (Supplementary Fig. 2).

PFD prevents stricture formation by inhibiting fibrosis

Esophageal strictures in the PFD-treated rats were significantly improved compared to those in the vehicle-treated rats on day 9 (55% vs. 81%, n = 8, $P < 0.01$) (Fig. 2C, 2D). In addition, mean thickness and fibrotic areas of the PFD-treated rats were significantly lower than those of the vehicle-treated rats on day 9, respectively (491 μm vs. 666 μm, n

= 8, P <0.01) (64% vs. 43%, n = 8, P <0.01) (Fig. 2E-G). The thickness and fibrotic areas on day 6 showed similar dynamics as those on day 9 (Supplementary Figure 3A-C).

PFD suppresses the activation of the NLRP3 inflammasome and the expression of fibrosis-related molecules

Compared with the vehicle treatment, PFD treatment significantly reduced the mRNA expression of IL-1β (Fig. 3A), NLRP3 (Fig. 3B), caspase-1 (Fig. 3C), and the fibrosis-related genes TGF-β1 (Fig. 3E) and COL1A1 (Fig. 3F) on day 6 after ulcer induction. The mRNA levels of inflammatory cytokines such as IL-18 (Fig. 3D), TNF-α (Supplementary Fig. 4A), and IL-6 (Supplementary Fig. 4B) did not significantly differ between the PFD- and vehicle-treated rats (n = 8). Consistent with the PCR results of mRNA expression levels, esophageal ulceration increased the protein levels of NLRP3, pro-caspase-1, cleaved caspase-1, pro-IL-1β, mature IL-1β, TGF-β1, and COL1A1 on day 6, and treatment with PFD inhibited the increase in the protein levels of these molecules (n = 6) (Fig. 3G).

Preventive effect of PFD on the expression and localization of cleaved caspase-1 in the ulcerated esophagus

The localization and expression of cleaved caspase-1 were determined using histological immunofluorescence. The results showed that cleaved caspase-1 was diffusely expressed in the submucosal granulation tissues of esophageal ulcers in the vehicle-treated rats on day 6, whereas the rats treated with PFD exhibited a considerable decrease in cleaved caspase-1 expression (Fig. 4A). Double staining of cleaved caspase-1 and CD68 demonstrated that the majority of the cells expressing cleaved caspase-1 were macrophages and monocytes (Fig. 4B). In normal esophageal tissues of the non-treated rats, cleaved caspase-1 was not expressed, and CD68 was slightly expressed (Fig. 4C).

IL-1β supplementation abolishes the beneficial effects of PFD against ulcer healing and its protective effects against stricture formation

To investigate the role of PFD and IL-1β, a product of NLRP3 activation, in esophageal stricture after ulcer healing, the rats were administered vehicle or intraperitoneally injected rat recombinant IL-1β (0.1 μg/kg) starting 3 days after ulcer induction. The administration of recombinant IL-1β abolished the beneficial effects of PFD against esophageal ulcer healing on day 6 (Fig. 5A, B) and reduced its preventive effect against esophageal stricture formation after healing of the ulcer on day 9 (n = 6) (Fig.5C, D). However, IL-1β supplementation did not affect ulcer healing (Fig. 5A, B) or the severity of esophageal stricture (Fig. 5C, D) in the vehicle-treated rats (n = 6).

Inhibition of the NLRP3 inflammasome enhanced ulcer healing and prevented stricture formation by inhibiting fibrosis

To confirm the involvement of the NLRP3/caspase-1/IL-1β axis in the suppressive effects of PFD, glyburide (NLRP3 inhibitor) and ac-YVAD-cmk (caspase-1 inhibitor) were administered. The esophageal ulcer area in the glyburide- and ac-YVAD-cmk-treated rats was significantly lower than that in the vehicle-treated rats on day 6 (n = 6) (Fig. 6A, B). Similarly, glyburide and ac-YVAD-cmk significantly reduced the esophageal stricture rate on day 9 (Fig. 6C, D) and reduced the thickness and fibrotic areas on day 9 (Fig. 6E-G). Moreover, similar to the PFD treatment results, both treatments significantly inhibited the protein levels of cleaved caspase-1, mature IL-1β, TGF-β1, and COL1A1 on day 6 (n = 6) (Fig. 6H).

Discussion

Here, we demonstrated that treatment with PFD promoted acetic acid-induced ulcer healing; attenuated fibrosis by suppressing the increase in the expression of NLRP3,

cleaved caspase-1, and mature IL-1β proteins; and prevented esophageal stricture formation. Interestingly, the expression of IL-18, which is also activated by inflammasomes, did not increase during the experiment. The administration of a low dose of exogenous IL-1β, which did not affect ulcer healing and stricture formation in the vehicle-treated rats, abolished the therapeutic effects of PFD on ulcer healing and its preventive effects on stricture formation. These results suggest that the promotion of ulcer healing and attenuation of stricture formation by PFD is related to a deficiency in the mature form of IL-1β. Furthermore, similar to PFD treatment, treatment with NLRP3 and caspase-1 inhibitors promoted ulcer healing and attenuated stricture formation by suppressing the increase in the expression of cleaved caspase-1 and mature IL-1β proteins. Collectively, these findings clearly indicate that the preventive effects of PFD against esophageal stricture formation after ulcer healing are mediated through the inhibition of IL-1β produced by NLRP3 inflammasomes. To the best of our knowledge, this is the first study to demonstrate that PFD can offer effective prophylaxis for esophageal stricture after ulcer healing through a novel mechanism of suppressing NLRP3 inflammasome activation.

Esophageal stricture formation after esophageal endoscopic treatment is a major clinical problem;[4–8] however, there are a few good animal models to study this phenomenon. In esophageal stricture models of pigs and dogs, uniform ulcers are technically difficult to produce, and it is difficult to obtain sufficient accuracy for molecular studies in addition to various problems caused by the type of animal species.[9,10,34] The alkaline drinking model of rodents is suitable for studying the healing process at the molecular level;[16,35] however, it is difficult to obtain strictures of the same size, and the influence of the alkali on other organs is a concern because of the characteristics of the procedure. Therefore,

we improved the existing esophageal acetic acid-induced ulcer model and established a new rat model that can exhibit not only the healing process of the ulcer but also the condition of the esophageal stricture by adjusting the size of the ulcer. The advantage of this model over other models is that it was easy to create ulcers of the same size, enabling an objective evaluation of the degree of esophageal ulceration and stricture. Furthermore, this modified model showed a low death rate (90% of the rats survived during the experimental period) and a high success rate (esophageal stricture formation in all rats). We consider this model to be an optimal rodent model that can better mimic strictures after esophageal injury, including post-endoscopic treatment, than other experimental models. However, further studies are needed to apply the results of this animal study to clinical practice since the process of acetic acid-induced ulcer formation used in the study differs from that in the clinical situation.

Our findings concur with the results of recent studies in different animal models of fibrosis disorders in organs such as the kidney,[23] heart,[29] and lung,[27] where the fibrosis and expression of fibrosis-related molecules were inhibited by PFD via the inhibition of NLRP3 inflammasome activation. Furthermore, PFD has been shown to prevent gastrointestinal stricture formation in esophageal burn models and inflammatory bowel disease models by inhibiting the expression of fibrosis-related molecules, including TGF-β1 and collagen I.[16,25,26] The TGF-β pathway is important in virtually all types of fibrosis, including esophagus fibrosis.[9,12] TGF-β binds to its cognate cell surface receptors, initiating downstream signaling that ultimately leads to nuclear translocation of the transcriptional modulators Smad2/3.[12] This leads to myofibroblast differentiation and increased expression of target genes that function to further enhance the production and secretion of extracellular matrix proteins such as collagen I, laminin, and fibronectin.[12]

This chain of events, in turn, causes physical organ deformation, which impairs organ function.[12] Here, we demonstrated that PFD, as well as NLRP3 and caspase-1 inhibitors, attenuated fibrosis during ulcer healing by inhibiting IL-1β, TGF-β1, and COL1A1 expression. A recent study showed that NLRP3 inflammasome activation could trigger fibrosis through TGF-β1 produced by IL-1β.[36,37] IL-1β acts as an autocrine signal in the fibroblast to upregulate mitogen-activated protein kinase family signaling pathways, resulting in increased gene expression of TGF-β1.[38] These findings suggest that PFD may prevent esophageal fibrosis by mediating the NLRP3/IL-1β/TGF-β1 axis (Fig. 7). However, the mechanism by which PFD prevents esophageal fibrosis remains unclear, and the anti-fibrotic effect of PFD has been attributed to the suppression of not only NLRP3 inflammasome activation but also various cell growth factors and the epithelial-mesenchymal transition.[39–41] These other mechanisms may be involved in the preventive effect of PFD on esophageal stricture.

NLRP3 inflammasome activation in the esophagus has been evaluated in only a few studies. Although recent studies, including ours, have demonstrated overactivation of the NLRP3 inflammasome in Barrett's epithelial cells,[42] Barrett's cancers,[43] and esophageal squamous cell carcinoma,[44] the role of the NLRP3 inflammasome in esophageal ulcers has not been reported. Here, we demonstrated that both NLRP3 and caspase-1 inhibitors prevented esophageal stricture formation by inhibiting fibrosis, suggesting that the NLRP3 inflammasome may play an important role in fibrosis in the esophagus, and this pathway may represent an attractive target for esophageal stricture.

In conclusion, we demonstrated that PFD promoted esophageal ulcer healing and prevented stricture formation via the inhibition of IL-1β produced by the NLRP3 inflammasome and expression of fibrosis-related molecules. As PFD has been clinically

used for many patients with idiopathic pulmonary fibrosis, its safety and tolerability have already been established. Thus, PFD may be a good candidate drug for prophylaxis of esophageal strictures after esophageal injury, including post-endoscopic treatment.

References

1. Hoffman RS, Burns MM, Gosselin S. Ingestion of caustic substances. N Engl J Med. 2020;382(18):1739–48.

2. Fujiwara Y, Arakawa T. Epidemiology and clinical characteristics of GERD in the Japanese population. J Gastroenterol. 2009;44(6):518–34.

3. Fujiwara Y. Symptom-based diagnostic approach for eosinophilic esophagitis. J Gastroenterol. 2020;55(9):833–45.

4. Nagami Y, Shiba M, Ominami M, Sakai T, Minamino H, Fukunaga S, Sugimori S, Tanaka F, Kamata N, Tanigawa T, Yamagami H, Watanabe T, Tominaga K, Fujiwara Y, Arakawa T. Single locoregional triamcinolone injection immediately after esophageal endoscopic submucosal dissection prevents stricture formation. Clin Transl Gastroenterol. 2017;8(2):e75.

5. Ishihara R. Prevention of esophageal stricture after endoscopic resection. Dig Endosc. 2019;31(2):134–45.

6. Nagami Y, Ominami M, Shiba M, Sakai T, Fukunaga S, Sugimori S, Otani K, Hosomi S, Tanaka F, Taira K, Kamata N, Yamagami H, Tanigawa T, Watanabe T, Ishihara T, Yamamoto K, Fujiwara Y. Prediction of esophageal stricture in patients given locoregional triamcinolone injections immediately after endoscopic submucosal dissection. Dig Endosc. 2018;30(2):198–205.

7. Hanaoka N, Ishihara R, Takeuchi Y, Uedo N, Higashino K, Ohta T, Kanzaki H,

Hanafusa M, Nagai K, Matsui F, Iishi H, Tatsuta M, Ito Y. Intralesional steroid injection to prevent stricture after endoscopic submucosal dissection for esophageal cancer: a controlled prospective study. Endoscopy. 2012;44(11):1007–11.

8. Yamaguchi N, Isomoto H, Nakayama T, Hayashi T, Nishiyama H, Ohnita K, Takeshima F, Shikuwa S, Kohno S, Nakao K. Usefulness of oral prednisolone in the treatment of esophageal stricture after endoscopic submucosal dissection for superficial esophageal squamous cell carcinoma. Gastrointest Endosc. 2011;73(6):1115–21.

9. Honda M, Kobayashi H, Nakayama Y, Kawamura H, Todate Y, Matsunaga R, Yamaguchi H, Hamada K. The mechanism of esophageal stricture after endoscopic resection: histological and biomechanical evaluation in a canine model. Ann Cancer Res Ther. 2017;25(1):30–7.

10. Arao M, Ishihara R, Tonai Y, Iwatsubo T, Shichijyo S, Matsuura N, Nakahira H, Yamamoto S, Takeuchi Y, Higashino K, Uedo N, Nakatsuka S. Comparison of endo cut mode and forced coag mode for the formation of stricture after esophageal endoscopic submucosal dissection in an in vivo porcine model. Surg Endosc. 2018;32(6):2902–6.

11. ASGE Technology Committee, Maple JT, Abu Dayyeh BK, Chauhan SS, Hwang JH, Komanduri S, Manfredi M, Konda V, Murad FM, Siddiqui UD, Banerjee SEndoscopic submucosal dissection. Gastrointest Endosc. 2015;81(6):1311–25.

12. Rockey DC, Bell PD, Hill JA. Fibrosis--a common pathway to organ injury and failure. N Engl J Med. 2015;372(12):1138–49.

13. Chai J, Norng M, Tarnawski AS, Chow J. A critical role of serum response factor in myofibroblast differentiation during experimental oesophageal ulcer healing in rats. Gut. 2007;56(5):621–30.

14. Baatar D, Kawanaka H, Szabo IL, Pai R, Jones MK, Kitano S, Tarnawski AS.

Esophageal ulceration activates keratinocyte growth factor and its receptor in rats: implications for ulcer healing. Gastroenterology. 2002;122(2):458–68.

15. Komaki Y, Kanmura S, Sasaki F, Maeda H, Oda K, Arima S, Tanoue S, Nasu Y, Hashimoto S, Mawatari S, Tsubouchi H, Ido A. Hepatocyte growth factor facilitates esophageal mucosal repair and inhibits the submucosal fibrosis in a rat model of esophageal ulcer. Digestion. 2019;99(3):227–38.

16. Orozco-Perez J, Aguirre-Jauregui O, Salazar-Montes AM, Sobrevilla-Navarro AA, Lucano-Landeros MS, Armendáriz-Borunda J. Pirfenidone prevents rat esophageal stricture formation. J Surg Res. 2015;194(2):558–64.

17. Tominaga K, Arakawa T, Kim S, Iwao H, Kobayashi K. Increased expression of transforming growth factor-beta1 during gastric ulcer healing in rats. Dig Dis Sci. 1997;42(3):616–25.

18. Tominaga K, Arakawa T, Watanabe T, Tanaka M, Takaishi O, Fujiwara Y, Fukuda T, Higuchi K, Kim S, Yamasaki K, Iwao H, Kobayashi K, Kuroki T. Increased mRNA levels of transforming growth factor-beta1 and monocyte chemoattractant protein-1 in ulcer relapse caused by interleukin-1beta in rats. Dig Dis Sci. 1998;43(9)(Suppl):134S–8S.

19. Yi YS. Functional crosstalk between non-canonical caspase-11 and canonical NLRP3 inflammasomes during infection-mediated inflammation. Immunology. 2020;159(2):142–55.

20. Liang Q, Cai W, Zhao Y, Xu H, Tang H, Chen D, Qian F, Sun L. Lycorine ameliorates bleomycin-induced pulmonary fibrosis via inhibiting NLRP3 inflammasome activation and pyroptosis. Pharmacol Res. 2020;158:104884.

21. Wree A, Eguchi A, McGeough MD, Pena CA, Johnson CD, Canbay A, Hoffman

HM, Feldstein AE. NLRP3 inflammasome activation results in hepatocyte pyroptosis, liver inflammation, and fibrosis in mice. Hepatology. 2014;59(3):898–910.

22. Pinar AA, Scott TE, Huuskes BM, Tapia Cáceres FE, Kemp-Harper BK, Samuel CS. Targeting the NLRP3 inflammasome to treat cardiovascular fibrosis. Pharmacol Ther. 2020;209:107511.

23. Kim YG, Kim SM, Kim KP, Lee SH, Moon JY. The role of inflammasome-dependent and inflammasome-independent NLRP3 in the kidney. Cells. 2019;8(11).

24. Taniguchi H, Ebina M, Kondoh Y, Ogura T, Azuma A, Suga M, Taguchi Y, Takahashi H, Nakata K, Sato A, Takeuchi M, Raghu G, Kudoh S, Nukiwa T, Pirfenidone Clinical Study Group in Japan. Pirfenidone in idiopathic pulmonary fibrosis. Eur Respir J. 2010;35(4):821–9.

25. Li G, Ren J, Hu Q, Deng Y, Chen G, Guo K, Li R, Li Y, Wu L, Wang G, Gu G, Li J. Oral pirfenidone protects against fibrosis by inhibiting fibroblast proliferation and TGF-β signaling in a murine colitis model. Biochem Pharmacol. 2016;117:57–67.

26. Kurahara LH, Hiraishi K, Hu Y, Koga K, Onitsuka M, Doi M, Aoyagi K, Takedatsu H, Kojima D, Fujihara Y, Jian Y, Inoue R. Activation of myofibroblast TRPA1 by steroids and pirfenidone ameliorates fibrosis in experimental Crohn's disease. Cell Mol Gastroenterol Hepatol. 2018;5(3):299–318.

27. Li Y, Li H, Liu S, Pan P, Su X, Tan H, Wu D, Zhang L, Song C, Dai M, Li Q, Mao Z, Long Y, Hu Y, Hu C. Pirfenidone ameliorates lipopolysaccharide-induced pulmonary inflammation and fibrosis by blocking NLRP3 inflammasome activation. Mol Immunol. 2018;99:134–44.

28. Sharawy MH, Serrya MS. Pirfenidone attenuates gentamicin-induced acute kidney injury by inhibiting inflammasome-dependent NLRP3 pathway in rats. Life Sci.

2020;260:118454.

29. Wang Y, Wu Y, Chen J, Zhao S, Li H. Pirfenidone attenuates cardiac fibrosis in a mouse model of TAC-induced left ventricular remodeling by suppressing NLRP3 inflammasome formation. Cardiology. 2013;126(1):1–11.

30. Tsuji H, Fuse Y, Kawamoto K, Fujino H, Kodama T. Healing process of experimental esophageal ulcers induced by acetic acid in rats. Scand J Gastroenterol Suppl. 1989;162:6–10.

31. Schneider CA, Rasband WS, Eliceiri KW. NIH Image to ImageJ: 25 years of image analysis. Nat Methods. 2012;9(7):671–5.

32. Higashimori A, Watanabe T, Nadatani Y, Nakata A, Otani K, Hosomi S, Tanaka F, Kamata N, Taira K, Nagami Y, Tanigawa T, Fujiwara Y. Role of nucleotide binding oligomerization domain-like receptor protein 3 inflammasome in stress-induced gastric injury. J Gastroenterol Hepatol. 2021;36(3):740–50.

33. Otani K, Watanabe T, Shimada S, Takeda S, Itani S, Higashimori A, Nadatani Y, Nagami Y, Tanaka F, Kamata N, Yamagami H, Tanigawa T, Shiba M, Tominaga K, Fujiwara Y, Arakawa T. Colchicine prevents NSAID-induced small intestinal injury by inhibiting activation of the NLRP3 inflammasome. Sci. Rep.:32587. Sci Rep. 2016;6:32587.

34. Yang K, Cao J, Yuan TW, Zhu YQ, Zhou B, Cheng YS. Silicone-covered biodegradable magnesium stent for treating benign esophageal stricture in a rabbit model. World J Gastroenterol. 2019;25(25):3207–17.

35. Erbaş M, Kiraz HA, Küçük A, Topaloğlu N, Erdem H, Şahin H, Toman H, Ozkan MT. Effects of tenoxicam in experimental corrosive esophagitis model. Dis Esophagus. 2015;28(3):253–7.

36. Zhang LL, Huang S, Ma XX, Zhang WY, Wang D, Jin SY, Zhang YP, Li Y, Li X. Angiotensin (1–7) attenuated angiotensin II-induced hepatocyte EMT by inhibiting NOX-derived H2O2-activated NLRP3 inflammasome/IL-1β/Smad circuit. Free Radic Biol Med. 2016;97:531–43.

37. Doerner AM, Zuraw BL. TGF-beta1 induced epithelial to mesenchymal transition (EMT) in human bronchial epithelial cells is enhanced by IL-1beta but not abrogated by corticosteroids. Respir Res. 2009;10(1):100.

38. Artlett CM. The role of the NLRP3 inflammasome in fibrosis. Open Rheumatol J. 2012;6:80–6.

39. Bai X, Nie P, Lou Y, Zhu Y, Jiang S, Li B, Luo P. Pirfenidone is a renal protective drug: mechanisms, signalling pathways, and preclinical evidence. Eur J Pharmacol. 2021;911:174503.

40. Fujiwara A, Shintani Y, Funaki S, Kawamura T, Kimura T, Minami M, Okumura M. Pirfenidone plays a biphasic role in inhibition of epithelial-mesenchymal transition in non-small cell lung cancer. Lung Cancer. 2017;106:8–16.

41. Ruwanpura SM, Thomas BJ, Bardin PG. Pirfenidone: molecular mechanisms and potential clinical applications in lung disease. Am J Respir Cell Mol Biol. 2020;62(4):413–22.

42. Nadatani Y, Huo X, Zhang X, Yu C, Cheng E, Zhang Q, Dunbar KB, Theiss A, Pham TH, Wang DH, Watanabe T, Fujiwara Y, Arakawa T, Spechler SJ, Souza RF. NOD-like receptor Protein 3 inflammasome priming and activation in Barrett's epithelial cells. Cell Mol Gastroenterol Hepatol. 2016;2(4):439–53.

43. Barber G, Anand A, Katarzyna Oficjalska O, Phelan JJ, Heeran AB, Flis E, Clarke NE, Watson JA, Strangmann J, Flood B, O'Neill H, O'Toole D, MacCarthy F,

Ravi N, Reynolds JV, Kay EW, Quante M, O'Sullivan J, Creagh EM. Characterizing caspase-1 involvement during esophageal disease progression. Cancer Immunol Immunother. 2020;69(12):2635–49.

44. Yu S, Yin JJ, Miao JX, Li SG, Huang CZ, Huang N, Fan TL, Li XN, Wang YH, Han SN, Zhang LR. Activation of NLRP3 inflammasome promotes the proliferation and migration of esophageal squamous cell carcinoma. Oncol Rep. 2020;43(4):1113–24.

Figure legends

Figure 1. Dynamics of esophageal ulcer healing and induction of stricture during ulcer healing

An esophageal ulcer was induced by applying 100% acetic acid to the serosa of the lower esophagus. (A, B) Time course of changes in esophageal ulcers during the ulcer healing process. (A) Representative macroscopic images of esophageal ulcers. (B) Ulcer area (mm^2) measured using a computerized image-analysis system. n = 8. (C) Fluoroscopic images of esophageal strictures following ulcer healing by esophagography on day 9. (D-F) Time course of representative histological changes determined by hematoxylin/eosin staining of esophageal ulcers during the ulcer healing process. EP: epithelium, SM: submucosal layer, MP: muscularis propria, GT: granulation tissue. The arrow indicates the epithelial cell migration. (G-L) Time courses of changes in mRNA expression of (G) interleukin (IL)-1β, (H) NLRP3, (I) caspase-1, (J) IL-18, (K) transforming growth factor (TGF)-β1, and (L) collagen type I alpha 1 chain (COL1A1) were determined using real-time quantitative reverse transcription-polymerase chain reaction (qRT-PCR). The expression levels of mRNA are expressed as a percentage of the mean values of the non-treated control rats. n = 8; $*P < 0.05$, $**P < 0.01$.

Figure 1

A

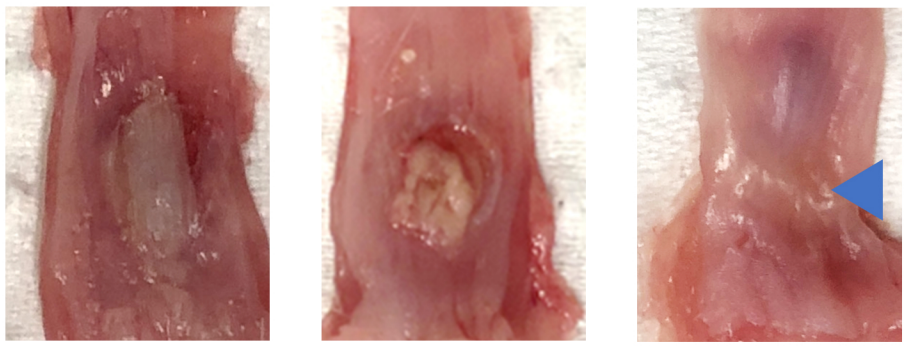

B

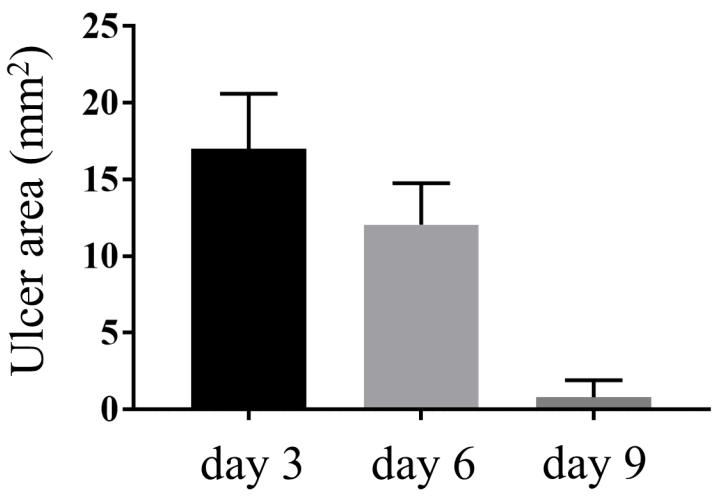

C

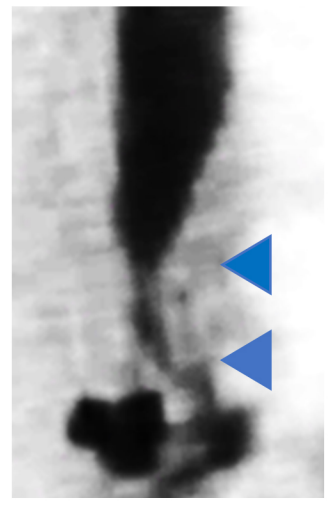

D

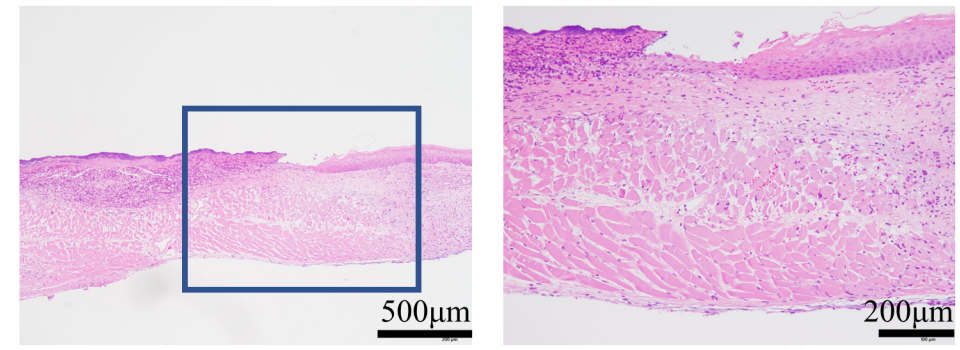

E

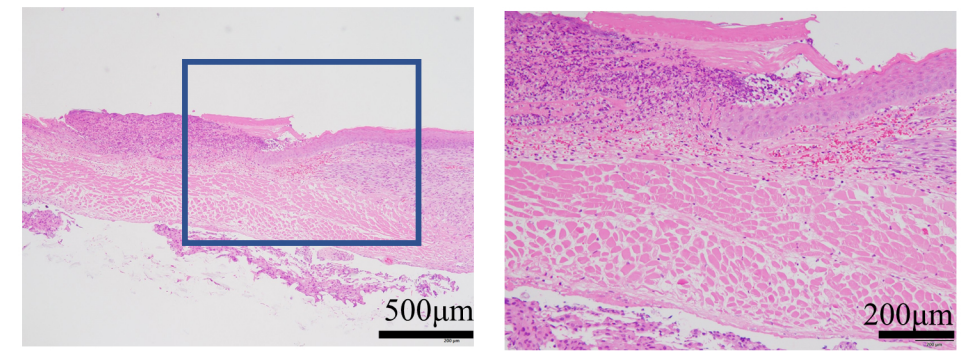

F

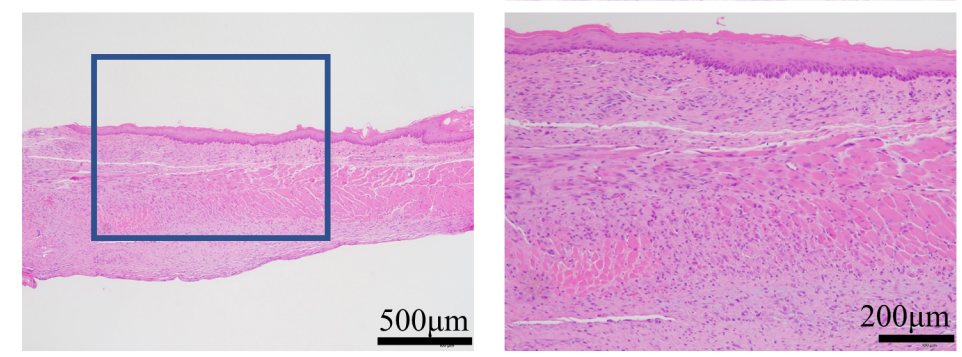

G

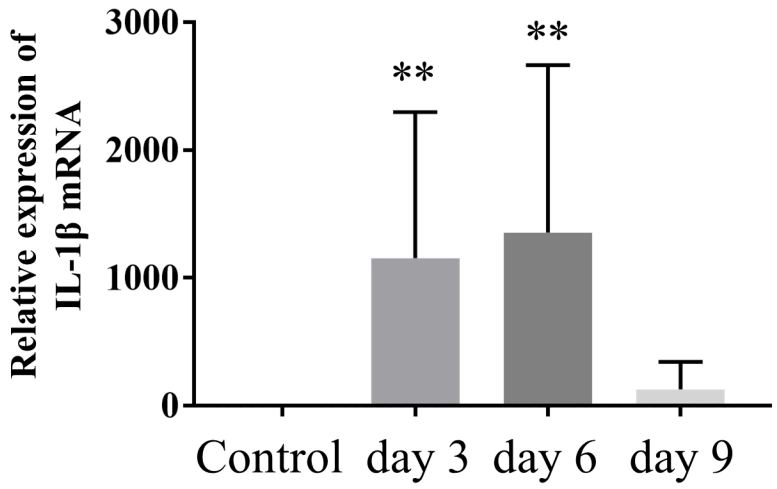

H

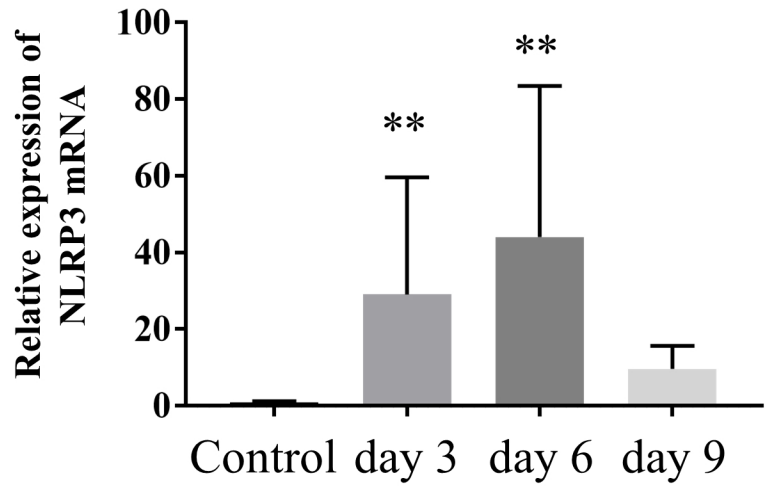

I

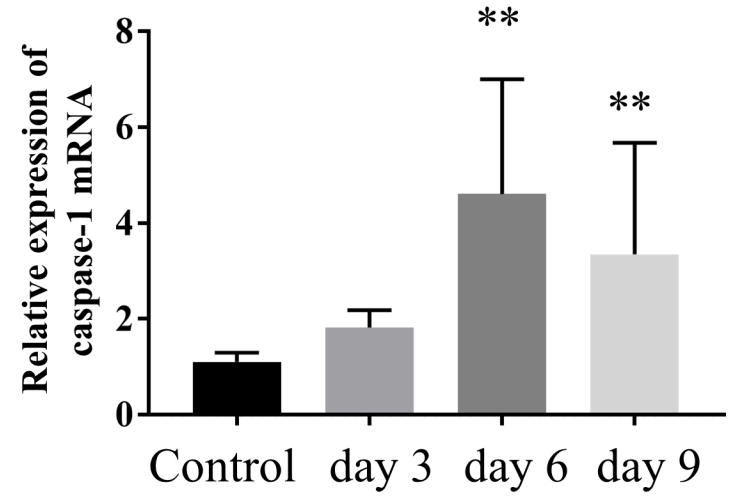

J

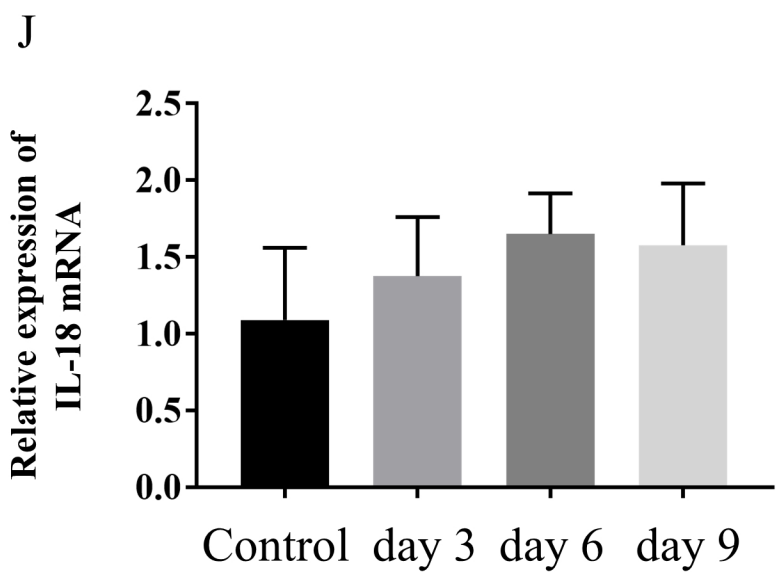

K

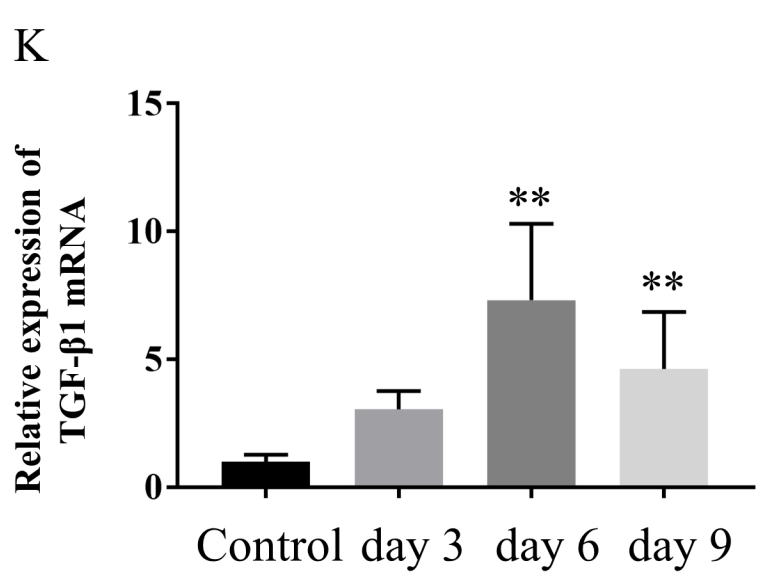

L

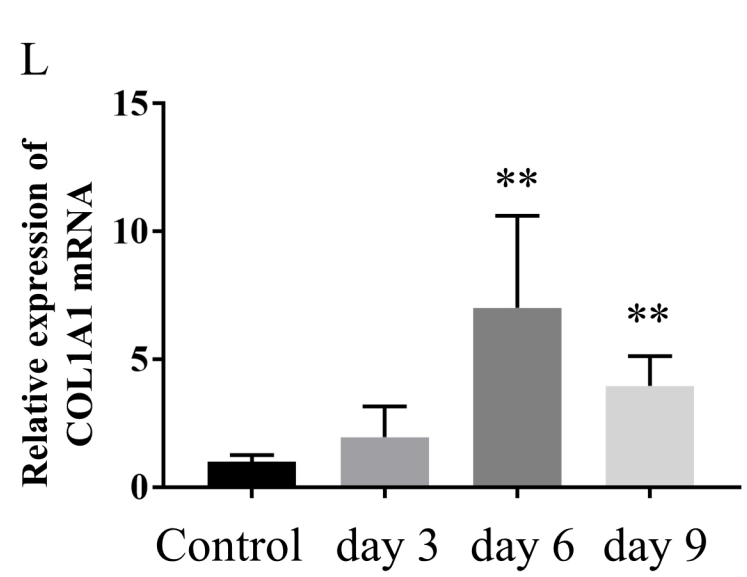

Figure 2. Pirfenidone (PFD) promotes esophageal ulcer healing and prevents stricture formation by inhibiting fibrosis

Rats with ulcers received intraperitoneal injections of PFD once daily from day 3. (A) Time course of changes in ulcer areas from day 6 to 9 with three doses of PFD: 100, 250, and 500 mg/kg. The ulcer area (mm^2) was measured using a computerized image-analysis system. (B) Time course of changes in the body weight (BW) of rats after ulcer induction with PFD at a dose of 500 mg/kg. n = 8. (C) Representative fluoroscopic images of esophageal stricture by esophagography on day 9 between the vehicle-treated and PFD-treated rats (500 mg/kg) and (D) comparison of the stricture rate (%). The stricture rate was calculated as 100 × (A – B) / A, where A is the largest diameter of the esophagus and B is the narrowest diameter of the esophagus after filling the esophagus with the contrast medium. n = 6. (E-G) Comparison of esophageal fibrosis by Masson trichrome staining on day 9 between the vehicle-treated and PFD-treated rats (500 mg/kg). n = 8. (E) Representative histological images, (F) thickness (μm) at the center of the ulcer, and (G) fibrotic area (%) measured as a percentage of blue-stained area using a computerized image-analysis system; n = 8; $*P < 0.05$, $**P < 0.01$.

Figure 2

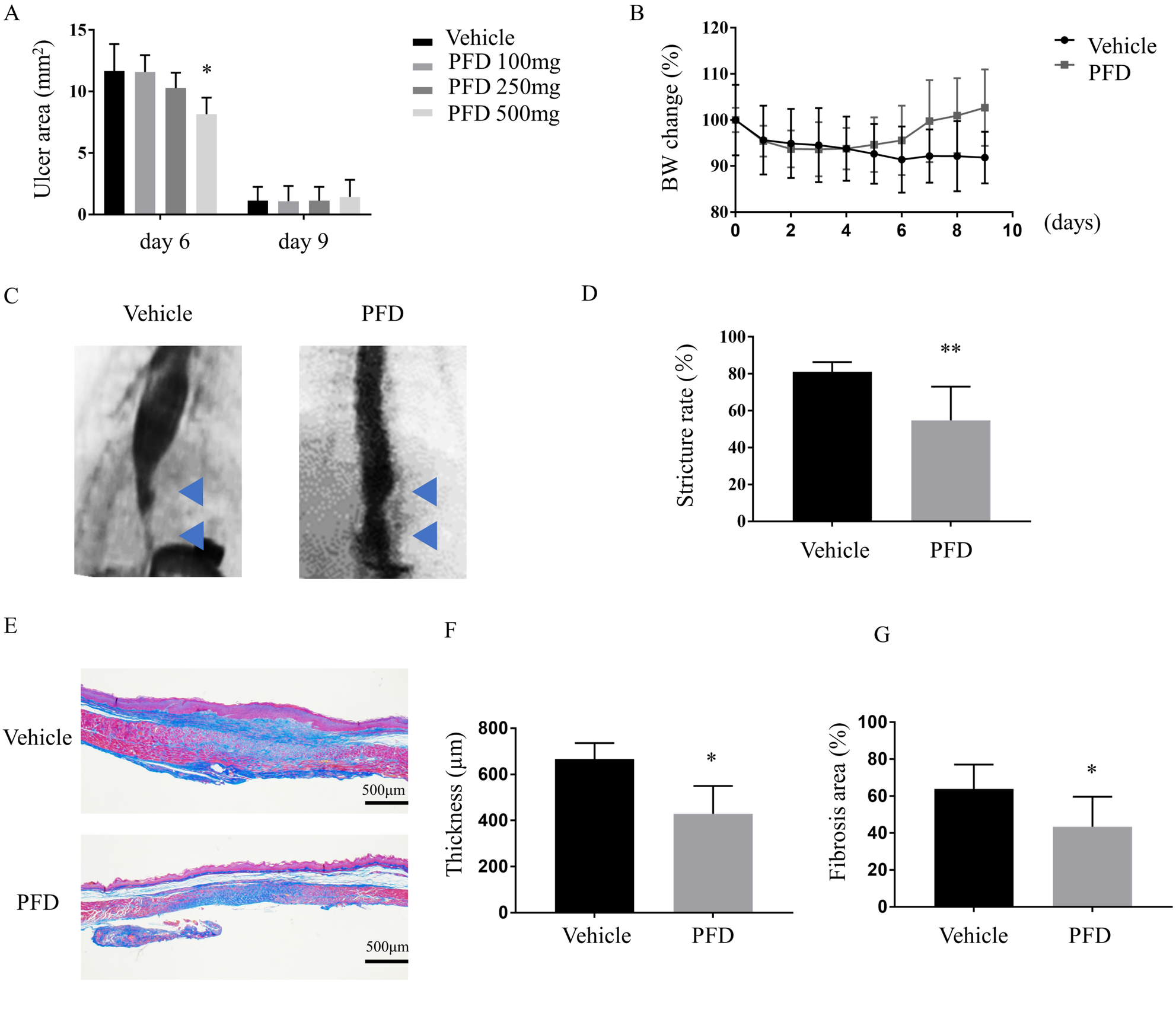
A
Ulcer area (mm²)
15
10
5
0
*
day 6
day 9
Vehicle
PFD 100mg
PFD 250mg
PFD 500mg
B
BW change (%)
120
110
100
90
80
0
2
4
6
8
10
(days)
Vehicle
PFD
C
Vehicle
PFD
D
Stricture rate (%)
100
80
60
40
20
0
**
Vehicle
PFD
E
Vehicle
PFD
500μm
500μm
F
Thickness (μm)
800
600
400
200
0
*
Vehicle
PFD
G
Fibrosis area (%)
100
80
60
40
20
0
*
Vehicle
PFD

Figure 3. PFD suppresses the activation of the NLRP3 inflammasome components and the expression of fibrosis-related molecules

Pirfenidone (500 mg/kg) or vehicle was intraperitoneally administered to rats once daily from 3 days after ulcer induction. (A-F) Comparison of expressions of mRNA of (A) IL-1β, (B) NLRP3, (C) caspase-1, (D) IL-18, (E) TGF-β1, and (F) COL1A1 determined using qRT-PCR between the vehicle-treated and PFD-treated rats on day 6. The mRNA levels are expressed as a percentage of the mean values of non-treated control rats. n = 8. (G) Representative images of western blots of NLRP3, pro-caspase 1, cleaved caspase-1, pro-IL-1β, mature IL-1β, TGF-β1, and COL1A1 on day 6. GAPDH was used as an internal control. n = 6; $*P < 0.05$, $**P < 0.01$.

Figure 3

A
Relative expression of IL-1β mRNA
6000
4000
2000
0
*
Vehicle
PFD
B
Relative expression of NLRP3 mRNA
150
100
50
0
*
Vehicle
PFD
C
Relative expression of caspase-1 mRNA
6
4
2
0
**
Vehicle
PFD
D
Relative expression of IL-18 mRNA
2.5
2.0
1.5
1.0
0.5
0.0
Vehicle
PFD
E
Relative expression of TGF-β1 mRNA
15
10
5
0
**
Vehicle
PFD
F
Relative expression of COL1A1 mRNA
10
8
6
4
2
0
**
Vehicle
PFD
G
Control
Vehicle
PFD
(kD)
NLRP3
118
Pro-caspase-1
45
Cleaved caspase-1
10
Pro-IL-1β
35
Mature IL-1β
17
TGF-β1
13
COL1A1
210
GAPDH
37

Figure 4. Preventive effect of PFD on the expression and localization of cleaved caspase-1 in the ulcerated esophagus

Pirfenidone (500 mg/kg) or vehicle was intraperitoneally administered to rats once daily from 3 days after ulcer induction. (A) Immunofluorescence detection of cleaved caspase-1 in the vehicle-treated and PFD-treated rats on day 6. (B, C) Double staining of cleaved caspase-1 and CD68 (B) in the PFD-treated rats on day 6 and (C) in untreated control rats.

Figure 4

Cleaved caspase-1

A

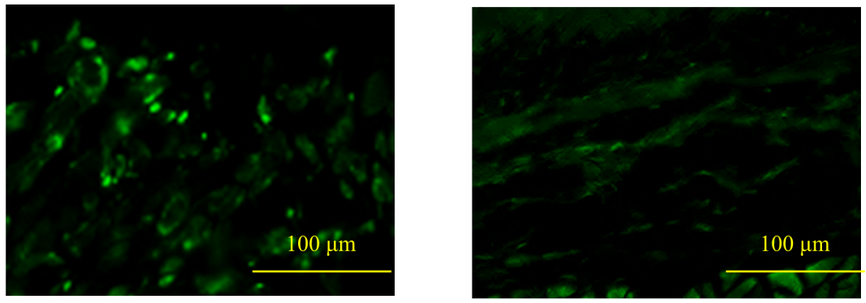

Vehicle PFD

B

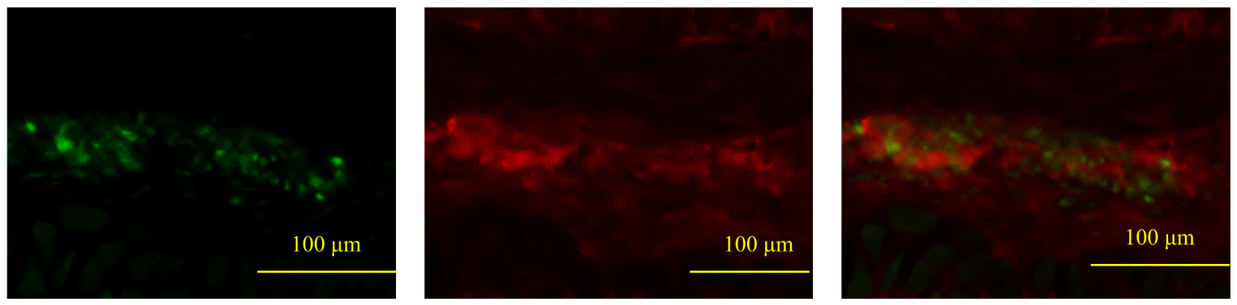

C

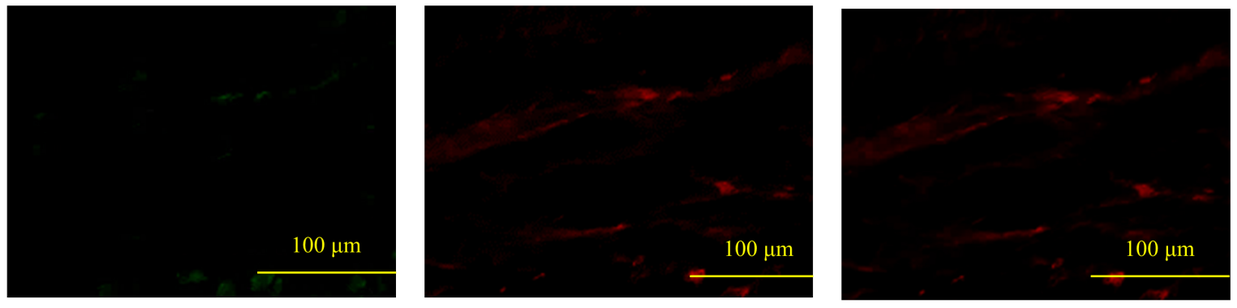

Cleaved caspase-1 CD68 Merge

Figure 5. IL-1β supplementation abolishes the therapeutic effect of PFD on ulcer healing and its preventive effects on stricture formation

PFD (500 mg/kg) and/or recombinant IL-β (0.1 μg/kg) were intraperitoneally administered to rats once daily from 3 days after ulcer induction. (A) Comparison of the ulcer areas on day 6. The ulcer area (mm^2) was measured using a computerized image-analysis system. n = 6. (B) Representative macroscopic images of the esophageal ulcer on day 6. (C) Comparison of the stricture rate (%) and (D) representative fluoroscopic images of esophageal strictures by esophagography on day 9. n = 6; $*P < 0.05$; n.s., not significant.

Figure 5

A

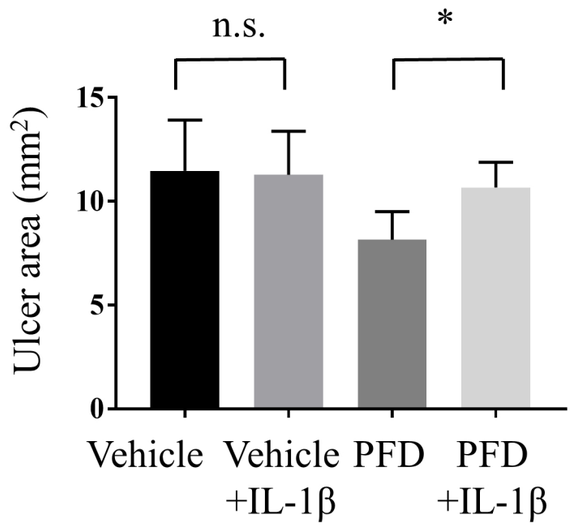

B

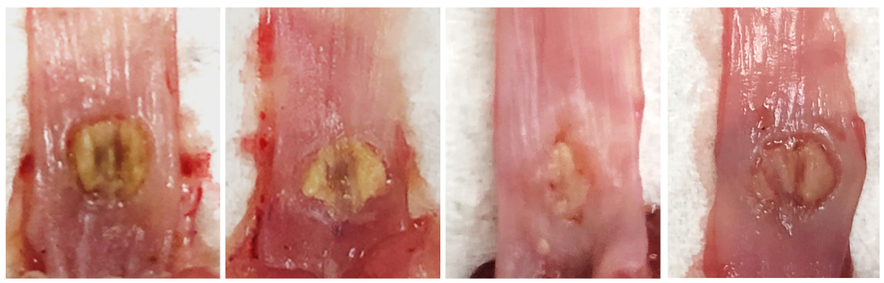

C

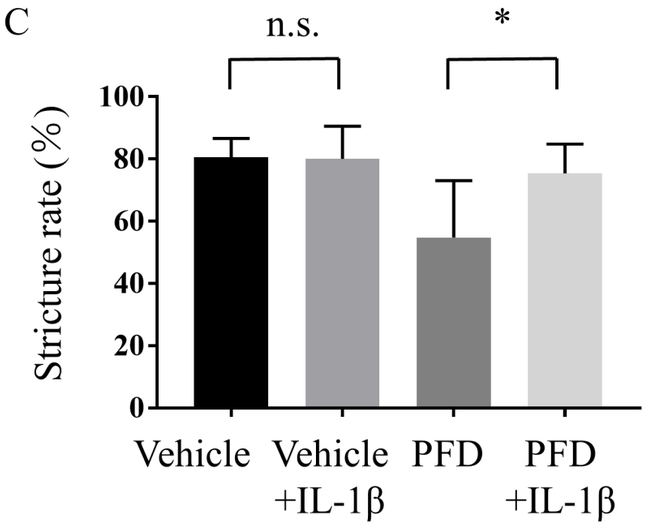

D

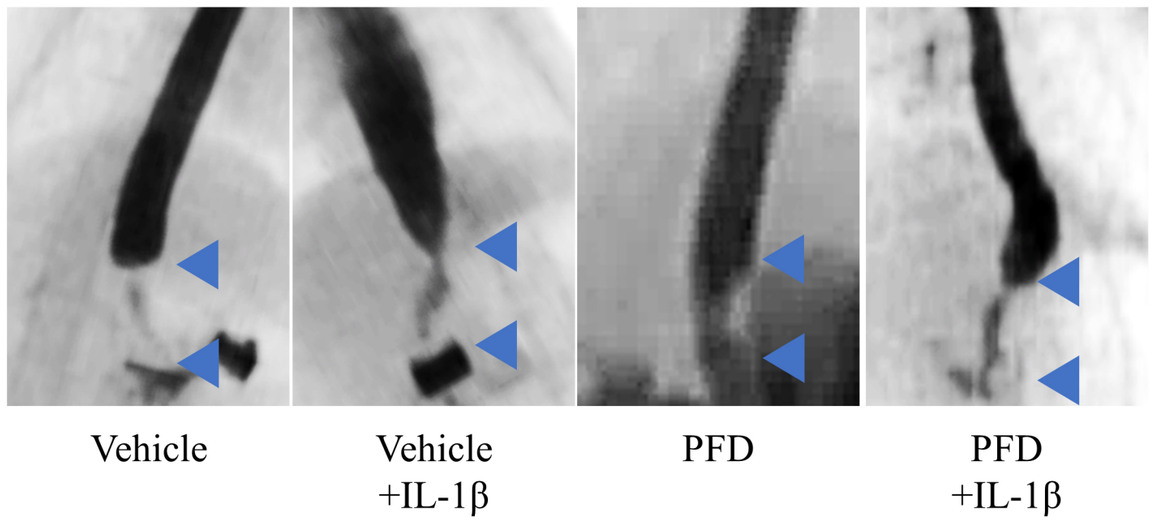

Figure 6. Inhibition of activation of the NLRP3 inflammasome promotes ulcer healing and prevents stricture formation by inhibiting fibrosis-related molecules

PFD (500 mg/kg), glyburide (10 mg/kg), or ac-YVAD-cmk (3 kg/kg) was intraperitoneally administered to rats once daily from 3 days after ulcer induction. (A) Comparison of the ulcer areas on day 6. The ulcer area (mm^2) was measured using a computerized image-analysis system. n = 6. (B) Representative macroscopic images of esophageal ulcers. (C) Comparison of the stricture rate (%) and (D) representative fluoroscopic images of esophageal strictures by esophagography on day 9. (E-G) Comparison of histological evaluations of esophageal fibrosis by Masson's trichrome staining. (E) Representative images, (F) thickness (μm) at the center of the ulcer, and (G) the fibrotic area (%). The fibrotic areas were measured as the percentage of blue-stained areas using a computerized image-analysis system. n = 6. (H) Representative images of western blots of cleaved caspase-1, mature IL-1β, TGF-β1, and COL1A1 on day 6. GAPDH was used as an internal control. n = 6; $*P < 0.05$.

Figure 6

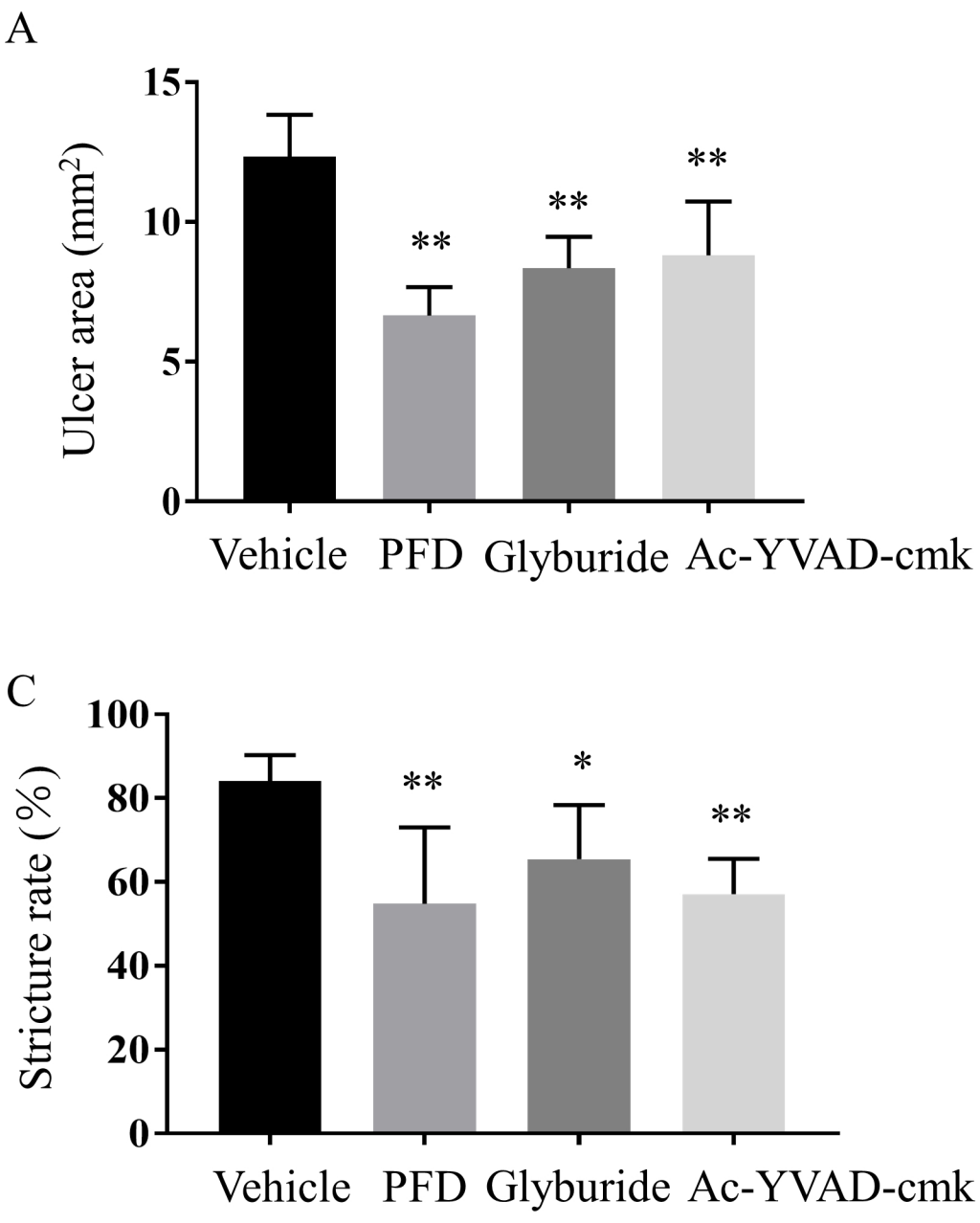
A
Ulcer area (mm2)
15
10
5
0
**
**
**
Vehicle
PFD
Glyburide
Ac-YVAD-cmk

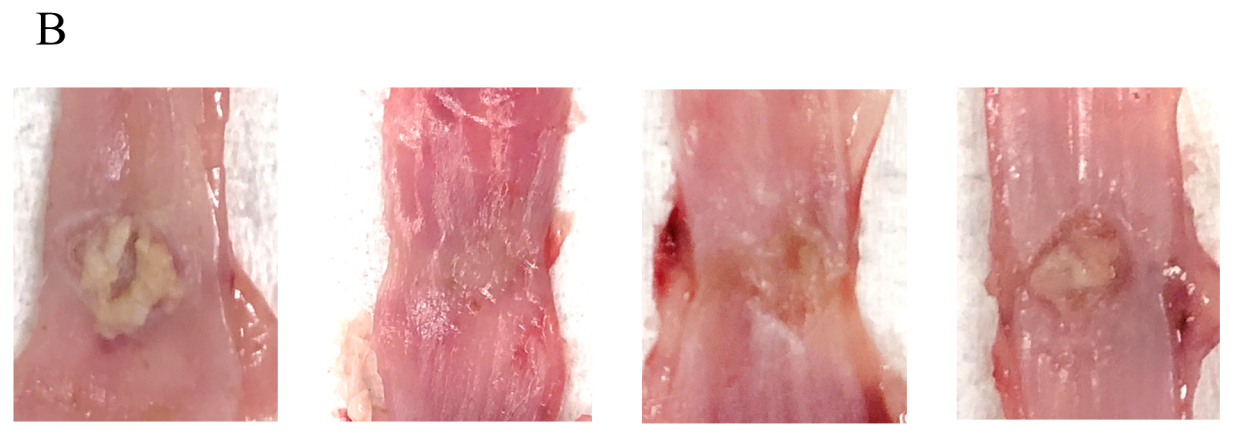
B
Vehicle
PFD
Glyburide
Ac-YVAD-cmk

C
Stricture rate (%)
100
80
60
40
20
0
**
*
**
Vehicle
PFD
Glyburide
Ac-YVAD-cmk

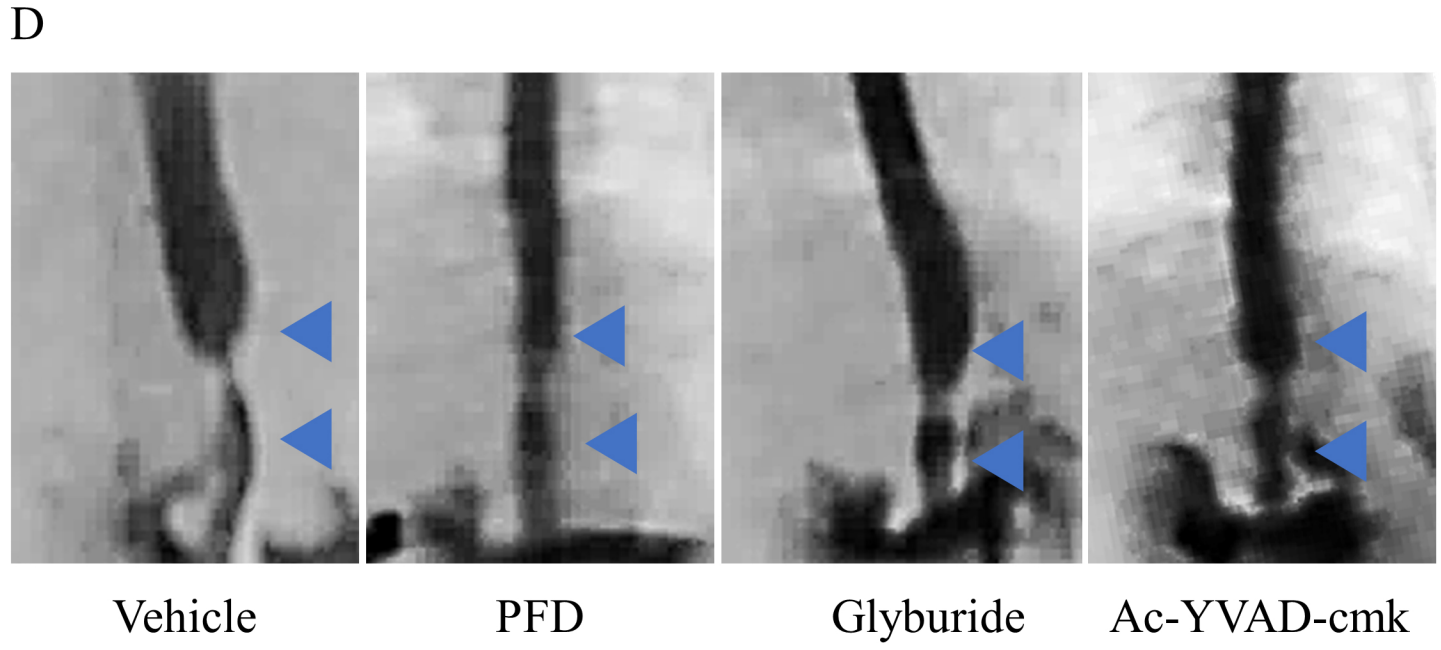
D
Vehicle
PFD
Glyburide
Ac-YVAD-cmk

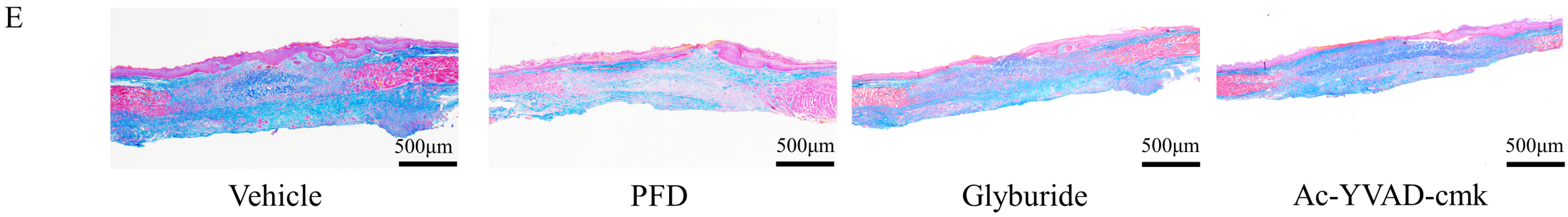
E
500μm
500μm
500μm
500μm
Vehicle
PFD
Glyburide
Ac-YVAD-cmk

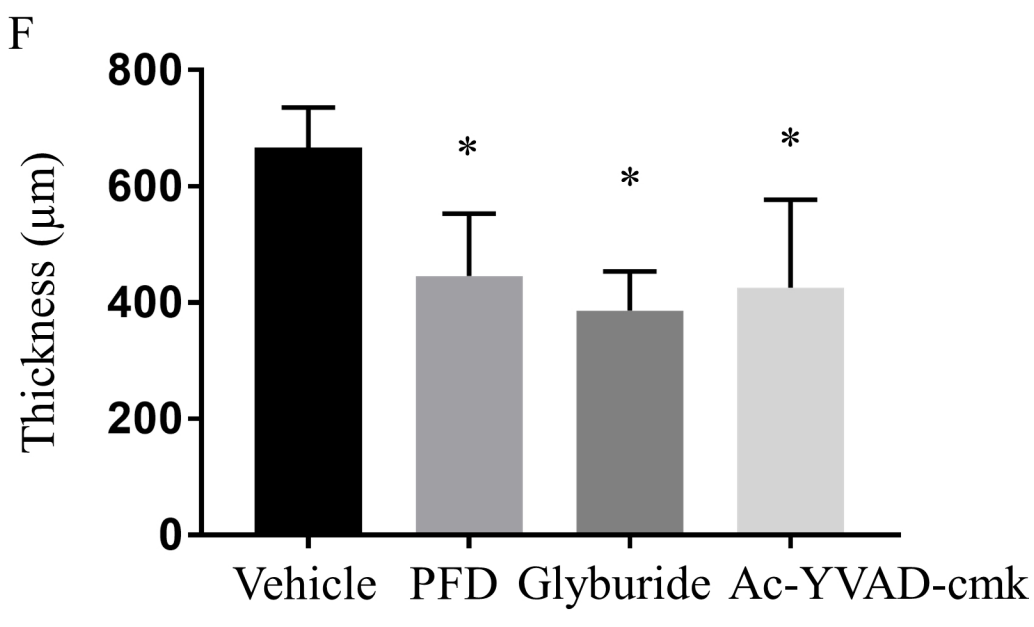
F
Thickness (μm)
800
600
400
200
0
*
*
*
Vehicle
PFD
Glyburide
Ac-YVAD-cmk

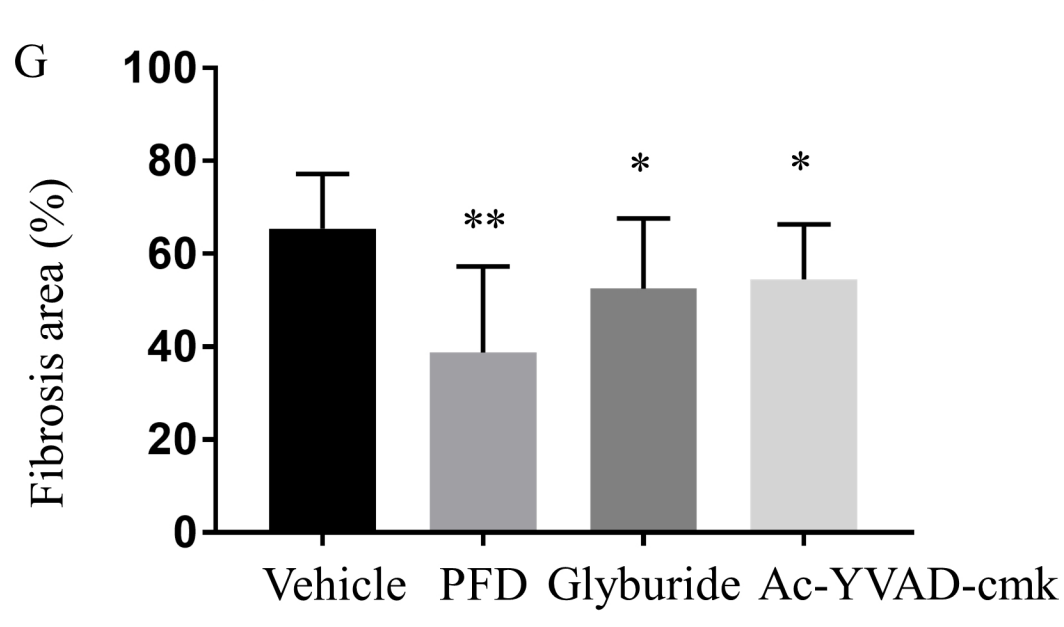
G
Fibrosis area (%)
100
80
60
40
20
0
**
*
*
Vehicle
PFD
Glyburide
Ac-YVAD-cmk

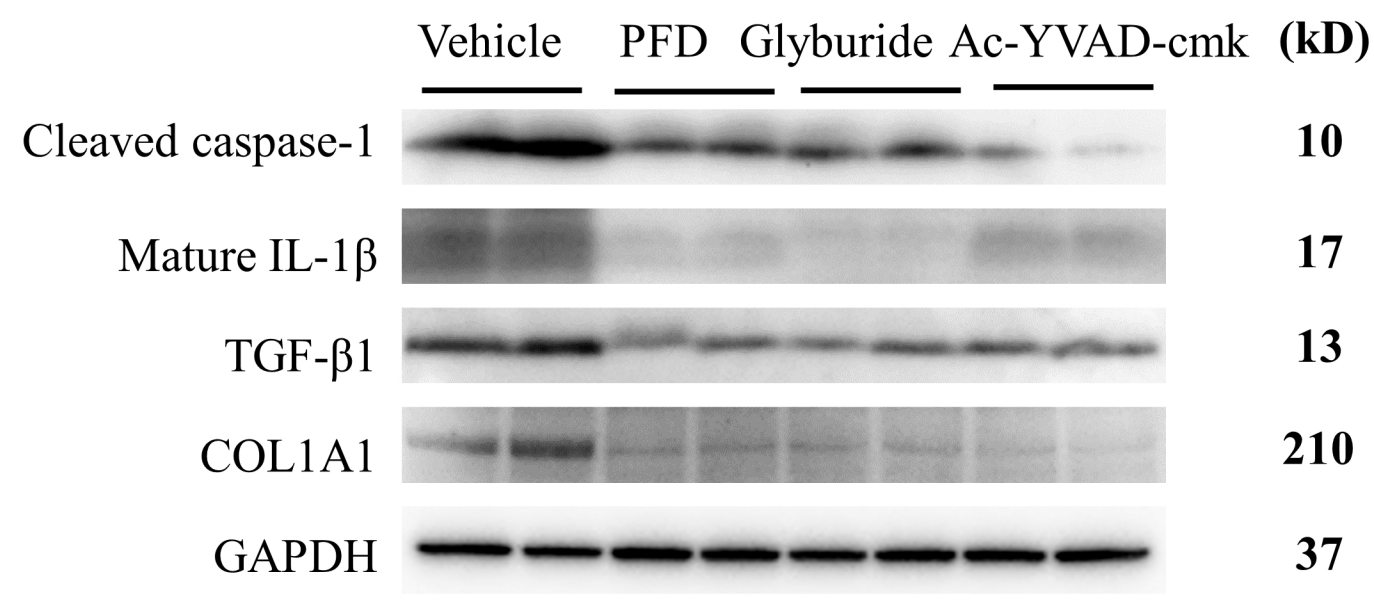
H
Vehicle
PFD
Glyburide
Ac-YVAD-cmk
(kD)
Cleaved caspase-1
10
Mature IL-1β
17
TGF-β1
13
COL1A1
210
GAPDH
37

Figure 7. Proposed mechanism underlying the protective effects of PFD on esophageal strictures after ulcer healing

NLRP3: nucleotide-binding and oligomerization domain-like receptor pyrin domain containing 3

ASC: Apoptosis-associated speck-like protein containing a CARD

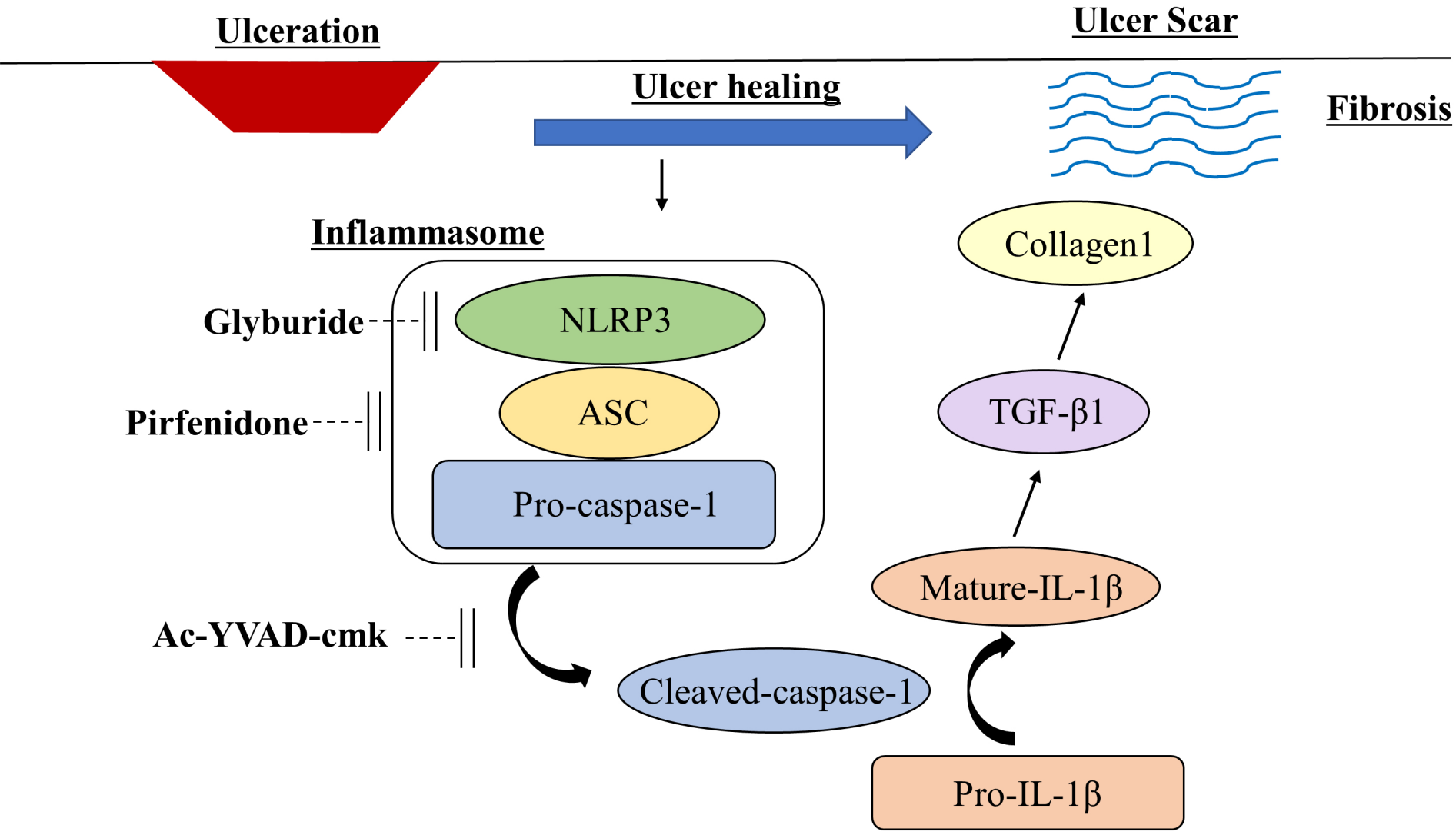
Ulceration
Ulcer Scar
Ulcer healing
Fibrosis
Inflammasome
Collagen1
Glyburide
NLRP3
Pirfenidone
ASC
TGF-β1
Pro-caspase-1
Mature-IL-1β
Ac-YVAD-cmk
Cleaved-caspase-1
Pro-IL-1β

Supplementary Figures

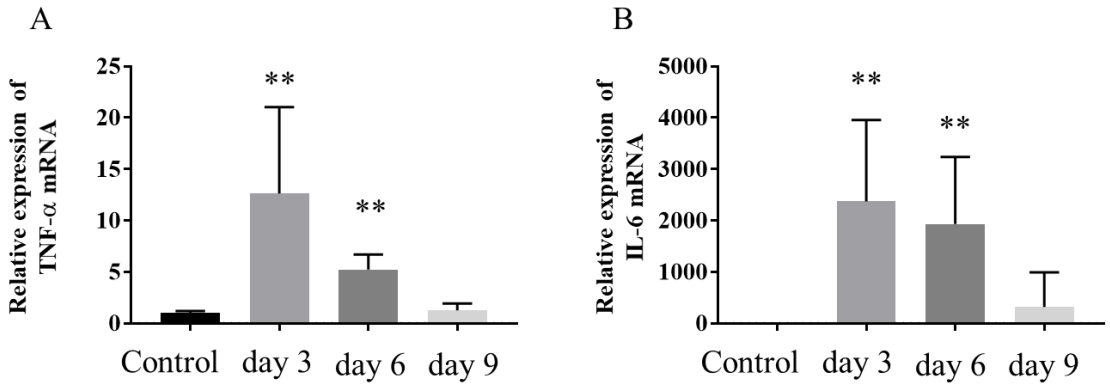

Supplementary Figure 1. Changes in mRNA expression during the acetic acid-induced ulcer healing

An esophageal ulcer was induced by applying 100% acetic acid to the serosa of the lower esophagus. (A, B) Time courses of changes in mRNA expression of tumor necrosis factor (TNF)-α (A) and interleukin (IL)-6 (B) were determined using qRT-PCR. The expression levels of mRNA are expressed as a percentage of the mean values of the non-treated control rats. n = 8; **P < 0.01.

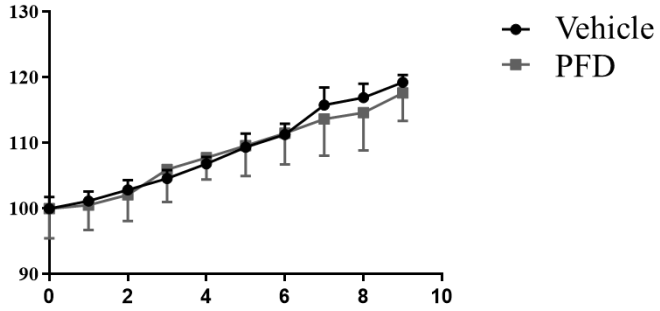

Supplementary Figure 2. Time course of changes in the body weight of untreated rats with PFD at a dose of 500 mg/kg. n = 6.

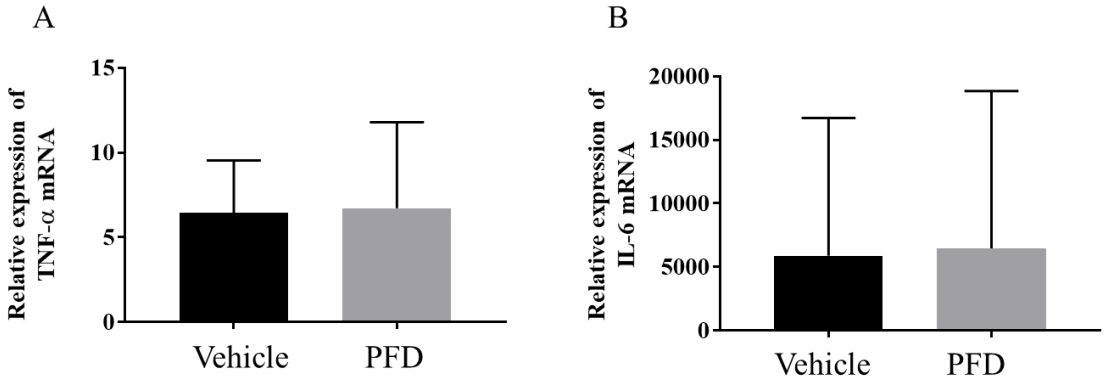

Supplementary Figure 3. Pirfenidone (PFD) suppresses expression of inflammatory cytokines

Pirfenidone (500 mg/kg) or vehicle was intraperitoneally administered to rats once daily from 3 days after ulcer induction. (A, B) Comparison of expressions of mRNA of (A) TNF-α and (B) IL-6 on day 6 between vehicle-treated rats and PFD-treated rats. The mRNA levels are expressed as a percentage of the mean values of non-treated control rats. n = 8.

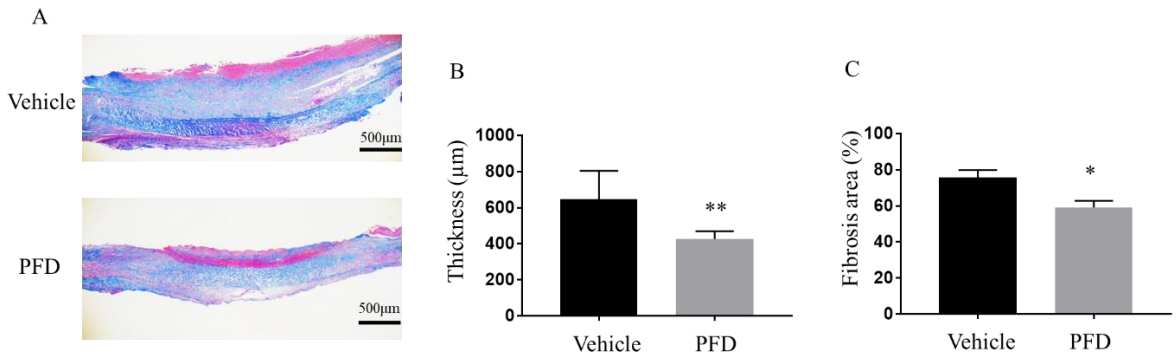

Supplementary Figure 4. Pirfenidone (PFD) inhibits fibrosis during ulcer healing process.

Comparison of esophageal fibrosis by Masson trichrome staining on day 9 between the vehicle-treated rats and PFD-treated rats (500 mg/kg). (A) Representative images, (B) thickness (μm) at the center of the ulcer, and (C) the fibrotic area (%). The fibrotic areas were measured as the percentage of blue-stained areas using a computerized image-analysis system. n = 8; *$P < 0.05$, **$P < 0.01$.

Supplementary Tables

Supplementary Table 1. The PCR primers and TaqMan probes

Gene Primer and probe

Primer names	**Sequence (5'->3')**
PCR	
Caspase-1 forward	GGTTGACACAATCTTTCAAATGATGA
Caspase-1 reverse	CCCTCTTCGGAGTTTCCTACTG
Caspase-1 Probe	FAM-CACCACTCCTTGTTTCTCTCCACGGCAT-TAMRA
COL1A1 forward	ACCGATGGATTCCAGTTCGAG
COL1A1 reverse	TGGACATCAGGCGAGGAA
COL1A1 Probe	FAM-ACATCGGCAGGATCGGAACCTTCGCT-TAMRA
IL-1β forward	AGTGGTATTCTCCATGAGCTTTGTA
IL-1β reverse	TGGGATCCACACTCTCCAGC
IL-1β Probe	FAM-AGAGACAAGCAACGACAAAATCCCTGTGGC-TAMRA
IL-6 forward	ACTCCATCTGCCCTTCAGGAA
IL-6 reverse	CAGTGGCTGTCAACAACATCAG
IL-6 Probe	FAM-CTCTCCGCAAGAGACTTCCAGCCAGT-TAMRA
IL-18 forward	ACCTGAAGATAATGGAGACTTGGAA
IL-18 reverse	CAACGAAGAGAACTTGGTCATTTATG
IL-18 Probe	FAM-CACTTTGGCAGACTTCACTGTACAACCGCA-TAMRA
NLRP3 forward	CCCAGTCTCCTTGCTGCG
NLRP3 reverse	CTGCAGTGTGACAAGATCAGAAC
NLRP3 Probe	FAM-CCACTCTGTGAGACAATGACTACCCCGAAA-TAMRA
TNF-α forward	AGAGCCCTTGCCCTAAGGACACCCCT
TNF-α reverse	TCATACCAGGGCTTGAGCTCA
TNF-α Probe	FAM-CACTTTGGCAGACTTCACTGTACAACCGCA-TAMRA
TGF-β1 forward	TGTCCGGCAGTGGCTGAA
TGF-β1 reverse	GGAGTACATTATCTTTGCTGTCACAA
TGF-β1 Probe	FAM-CACTGAAGCGAAGCGAAAGCCCTGTATTCCGTCTC-TAMRA

Supplementary Table 2. The list of the antibodies used

	Company	**Catalog No.**	**Dilution**	**note**
caspase-1	Santa Cruz Biotechnology	sc-56036	1:200	WB
Collagen 1	BIS	bs-10423R	1:500	
IL-1β	R&D Systems	AF501NA	1:1000	
NLRP3	Novus Biologocals	NBP2-12446	1:200	
TGF-β1	Abcam	ab215715	1:1000	
GAPDH	Sigma-Aldrich	G-8795	1:10,000	
CD68	Abcam	ab955	1:200	IF
cleaved caspase-1 p10	Cell Signaling Technology	Asp296	1:50	
Alexa Fluor® 488 Chicken Anti-rabbit IgG (H+L)	Thermo Fisher Scientific	A-21441	1:1,000	
Alexa Fluor® 546 Goat Anti-mouse IgG (H+L)	Thermo Fisher Scientific	A-11030	1:1,000	

WB, western blotting; IF, immunofluorescence.